RESEARCH ARTICLE

GENETIC EVOLUTION

Linking a mutation to survival in wild mice

Rowan D. H. Barrett[1]*†, Stefan Laurent[2]†‡, Ricardo Mallarino[3,4]†§, Susanne P. Pfeifer[5], Charles C. Y. Xu[1], Matthieu Foll[6], Kazumasa Wakamatsu[7], Jonathan S. Duke-Cohan[8], Jeffrey D. Jensen[5], Hopi E. Hoekstra[3,4]*

Adaptive evolution in new or changing environments can be difficult to predict because the functional connections between genotype, phenotype, and fitness are complex. Here, we make these explicit connections by combining field and laboratory experiments in wild mice. We first directly estimate natural selection on pigmentation traits and an underlying pigment locus, *Agouti*, by using experimental enclosures of mice on different soil colors. Next, we show how a mutation in *Agouti* associated with survival causes lighter coat color through changes in its protein binding properties. Together, our findings demonstrate how a sequence variant alters phenotype and then reveal the ensuing ecological consequences that drive changes in population allele frequency, thereby illuminating the process of evolution by natural selection.

Although a growing number of genomic studies have pinpointed genes that contribute to phenotypic evolution (*1*–*3*), often the ecological mechanisms driving trait evolution remain untested. On the other hand, field studies have documented the action of natural selection on traits (*4*–*6*), but the underlying molecular mechanisms are typically unknown. We combine a large-scale manipulative field experiment with laboratory-based genetic and biochemical tests to identify both the ecological and molecular mechanisms underlying trait adaptation in a wild vertebrate. Forging these mechanistic connections will aid in understanding the evolutionary consequences of environmental change in natural populations (*7*, *8*).

We took advantage of recently evolved, cryptically colored populations of deer mice (*Peromyscus maniculatus*) to investigate the genetic consequences of divergent natural selection. The Sand Hills of Nebraska were formed from light-colored quartz ~8,000 to 10,000 years ago (*9*). This dune habitat differs from the surrounding habitat in physical properties, most notably the soil color (*10*) (Fig. 1). Because the Sand Hills are geologically young and ecologically distinct, deer mouse populations inhabiting the area are expected to have recently evolved and strongly selected adaptations to this environment. One example of such an adaptation is pigmentation. The dorsal coats of deer mice are correlated with substrate color, with light mice occupying the light Sand Hills (*11*). The primary hypothesis for this phenotypic change is selection for crypsis against avian predators (*11*–*13*). Pigmentation differences between habitat types are associated with multiple mutations in *Agouti* (*14*, *15*), a locus that mediates the production of yellow pigment (pheomelanin) in vertebrates (*16*, *17*) and deer mice, specifically (*13*). Thus, Sand Hills deer mice and the *Agouti* locus are a useful system to directly test both the ecological and molecular mechanisms by which specific sequence variants alter phenotype and ultimately fitness.

Divergent selection on pigmentation in experimental enclosures

To explicitly test for selection that favors locally adapted pigment phenotypes, we collected 481 wild mice from the ancestral "dark" and derived "light" sites. We then introduced 75 to 100 individuals in equal proportions on the basis of the capture site (i.e., dark versus light) to each of six field enclosures (three in each habitat) that measured 50 m by 50 m and were devoid of native mice and terrestrial predators but open to avian predators (Fig. 1) (*18*). Among these founding individuals, we identified significant differences in five pigment traits (dorsal brightness, dorsal chroma, ventral brightness, ventral chroma, and tail pattern) between mice captured at dark versus light sites (all traits: $P < 0.001$) (fig. S1). Pigment phenotypes

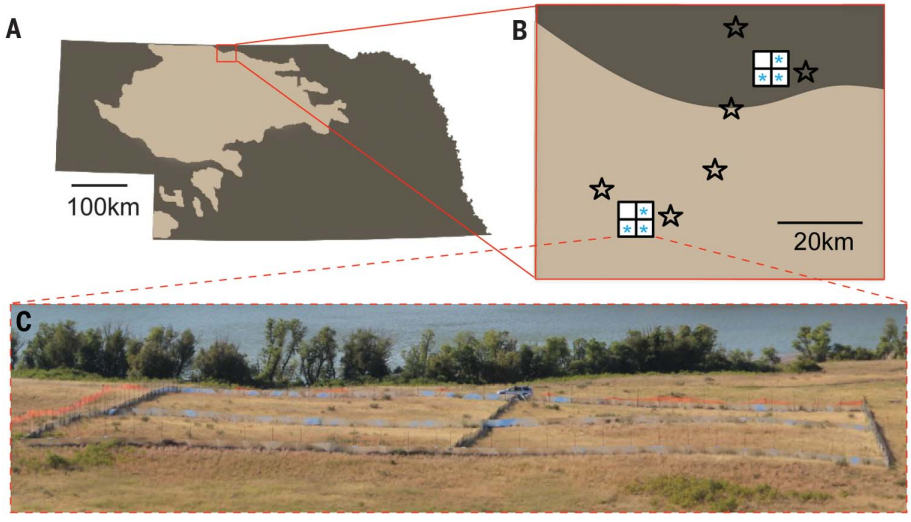

Fig. 1. Experimental site and environmental variation in the Sand Hills region of Nebraska. (**A**) Map of Nebraska showing the Sand Hills region (light color) and location of the enclosure experiment. (**B**) Map of the replicate enclosures (squares) and sampling locations for mice introduced to the enclosures (stars) used in the experiment (table S8). Light blue asterisks indicate the six enclosures used; we did not introduce mice to the fourth enclosure at either site. (**C**) Enclosures are shown at the light site in Sand Hills habitat (truck for scale). (**D** and **E**) Typical habitat is shown on the Sand Hills (D, light habitat) and off the Sand Hills (E, dark habitat); insets show typical soil substrate.

were largely independent, with weak and mostly insignificant correlations among traits [coefficient of determination (R^2) < 0.06 for all traits] (table S1), suggesting that these traits may be subjected to independent selection.

Using a mark-recapture approach, we tracked survival of these introduced individuals during five 2-week sampling periods over 14 months, by which time mortality reached 100% in most enclosures (Fig. 2, A and B), similar to mortality rates in the wild (*19*). Because sampling error is inversely proportional to the number of survivors, we focused our analyses on a comparison between the colonizing populations (time point 0) and survivors present at time point 1 (~3 months after the start of the experiment), when average survival rates were 45%. Regardless of sampling origin or phenotype, the survival rates were twice as high in dark enclosures relative to light enclosures (60% versus 30% at time point 1). Mice introduced to enclosures that matched the habitat type in which they were originally caught had greater survival than nonlocal mice (Fig. 2, A and B, and table S2) (*18*), suggesting local adaptation of populations from each environment type.

To explicitly test if pigmentation may be contributing to local adaptation, we tested for shifts in the distribution of pigment traits over time. We documented significant selection on pigmentation, primarily manifested through higher survival of mice with locally cryptic dorsal pigmentation [95% Bayesian credible intervals for the effect of the interaction between dorsal brightness and experimental treatment on survival do not contain zero (*18*)] (Fig. 2, C to F, and tables S2 and S3). In light enclosures, the surviving mice were, on average, 1.44 times lighter in dorsal color than the average mouse in the founding populations, whereas in dark enclosures, the average mouse was 1.98 times darker. Linear selection gradients for dorsal brightness were positive in all three light site enclosures and negative in all three dark site enclosures (one-sided t test of linear selection gradients in light versus dark enclosures: $t = -6.079$, df = 2.518, $P = 0.015$) (table S3). With the exception of ventral chroma in a single enclosure, no significant directional selection was detected on any other trait but dorsal brightness (tables S2 and S3). There was also no evidence for quadratic or correlational selection in the data (tables S4 and S5). Thus, divergent natural selection was likely acting on dorsal brightness between the two environment types.

Previous work with plasticine model mice suggests that avian predation is high in this region [~1% attack rates; (*14*)]. Moreover, owls are highly effective predators of mice and can discriminate between different color morphs even under moonlight conditions (*12*). During our field experiment, we observed owls hunting at the experimental sites (eight observations over 70 nights). Because the enclosures largely exclude other predators, we suggest that the significant association between dorsal brightness and survival

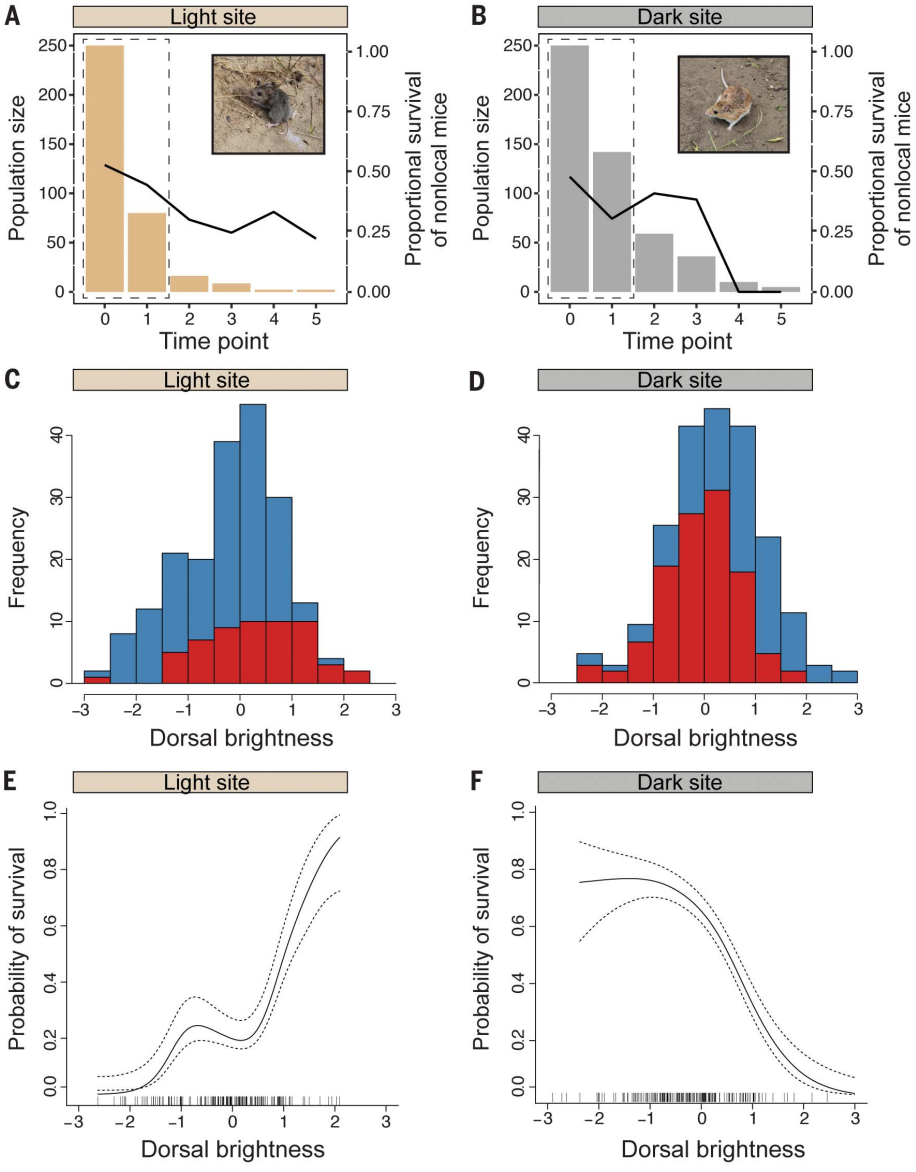

Fig. 2. Mortality and phenotypic change in the experimental populations. (**A** and **B**) Mortality in pooled enclosures at light (A) and dark (B) sites over five sequential episodes of selection (*18*). Bars represent the number of surviving individuals (independent of coat color) at each time point. Black lines represent the proportion of surviving individuals that were originally caught on the opposite habitat type of the enclosure type they were placed in (mice from dark habitat in light enclosures and mice from light habitat in dark enclosures). Conspicuously colored mice are shown on typical substrate at each experimental site. Dashed boxes denote the time period used in selection analyses. (**C** and **D**) Distributions of dorsal brightness at time point 0 (blue) and time point 1 (red) at the light (C) and dark (D) sites. (**E** and **F**) Visualizations of selection on dorsal brightness at the light (E) and dark (F) sites between time point 0 and 1. Cubic spline plots are generated from predicted values. The solid lines represent the fitted spline, and the dotted lines represent ±1 Bayesian SE.

[1]Redpath Museum and Department of Biology, McGill University, Montreal, Canada. [2]School of Life Sciences, Ecole Polytechnique Fédérale de Lausanne (EPFL), Lausanne, Switzerland. [3]Department of Organismic and Evolutionary Biology, Museum of Comparative Zoology, Harvard University, Cambridge, MA USA. [4]Department of Molecular and Cellular Biology, Howard Hughes Medical Institute, Harvard University, Cambridge, MA, USA. [5]School of Life Sciences, Center for Evolution and Medicine, Arizona State University, Tempe, AZ, USA. [6]International Agency for Research on Cancer, World Health Organization, Lyon, France. [7]Department of Chemistry, Fujita Health University School of Health Sciences, Toyoake, Japan. [8]Department of Medical Oncology, Dana-Farber Cancer Institute and Department of Medicine, Harvard Medical School, Boston, MA, USA.

***Corresponding author. Email: rowan.barrett@mcgill.ca (R.D.H.B.); hoekstra@oeb.harvard.edu (H.E.H.)** †These authors contributed equally to this work. ‡Present address: Department of Comparative Development and Genetics, Max Planck Institute for Plant Breeding Research, Cologne, Germany. §Present address: Department of Molecular Biology, Princeton University, Princeton, NJ, USA.

is likely driven by higher rates of avian predation on mice with conspicuous pigmentation.

The genetic consequences of selection on pigmentation

To investigate how selection on dorsal brightness impacts allele frequencies at the *Agouti* locus, we generated polymorphism data with enriched sequencing of (i) a 185-kb region that encompasses *Agouti* and all known regulatory elements and (ii) ~2100 unlinked genome-wide regions, each averaging 1.5 kb in length [following (*20*)], to control for demographic effects. In brief, we sequenced all 481 individuals and, after filtering, identified 2442 and 53,507 variable, high-quality sites in or near the *Agouti* gene and genome-wide, respectively. From these data, we observed greater changes in allele frequency at *Agouti* over time in the light than in the dark enclosures, consistent with higher mortality in light enclosures (Wilcoxon rank sum test: $W = 3{,}497{,}200$, $P < 0.001$) (fig. S2A).

To determine whether the changes in allele frequency at *Agouti* are best explained by selection or neutrality (i.e., random mortality), we calculated, for every *Agouti* variant site independently, the probability that the distribution of genotype frequencies observed in the survivors represents a random sample from the initial population (*18*). After 3 months, the surviving mice showed nonrandom genotype frequencies at 353 and 549 single-nucleotide polymorphisms (SNPs) in the light and dark enclosures, respectively (Fig. 3, A and B). To account for the large number of tests involved, we used a resampling procedure to determine how many SNPs would be expected to show significant changes by chance alone. In the light enclosures, the patterns of allele frequency change at *Agouti* SNPs could not be distinguished from neutrality (Fig. 3C), likely because of reduced statistical power caused by the low number of survivors. By contrast, in the dark enclosures, our results reject the null hypothesis, suggesting that the number of significant changes in allele frequency is incompatible with a strictly neutral model (Fig. 3D). Therefore, in the dark enclosures, we find allele frequency changes at the *Agouti* locus consistent with selection, and thus, patterns at the genetic level parallel the change observed at the phenotypic level.

Because there is no recombination between loci in a single generation, we further tested whether the large number of sites with significant allele frequency changes in the dark enclosures could be explained by correlated responses at loci linked to a limited number of SNPs under selection (*18*). From our phenotypic selection results, we a priori hypothesized that SNPs associated with dorsal brightness should be experiencing direct selection. Thus, for each of 31 *Agouti* SNPs associated with dorsal brightness (*15*), we compared genotype frequencies under a model with and without selection (*18*). Of these, seven SNPs, including six SNPs in or near regulatory regions of *Agouti* and a single amino acid deletion of serine at amino acid position 48 in exon 2 (ΔSer), had an allele frequency change that could not be explained solely by random sampling (Fig. 4A and table S6). Four of these seven SNPs also exhibited high levels of differentiation between mice originally captured from light and dark habitats (Fig. 4B and table S6). In addition, one regulatory SNP and the ΔSer have been associated with historical signals of positive selection in Sand Hills populations (*14*, *15*).

To test whether selection on each of these candidate variants could account for the observed number of SNPs with biased genotype frequencies in the survivors, we recalculated null distributions by assigning each candidate individually as our single selected target site. After correction for multiple testing, each of the seven could account for the observed change in genotype frequencies in the survivors (Fig. 4C). By contrast, a model using the SNP from the genome-wide control dataset with the most significant allele frequency change cannot explain the observed patterns (fig. S2B). Linkage disequilibrium (LD) analyses of the seven candidate variants identified three linkage blocks (fig. S2C): two sets of three physically proximate regulatory SNPs and the ΔSer, the latter displaying low LD with all other candidate SNPs (Fig. 4D). These data suggest that each of these three linkage blocks harbors variants directly responding to selection on dorsal brightness. Thus, selection on a limited number of genetic targets in the *Agouti* locus is likely sufficient to drive shifts in allele frequency and rapid change in phenotype.

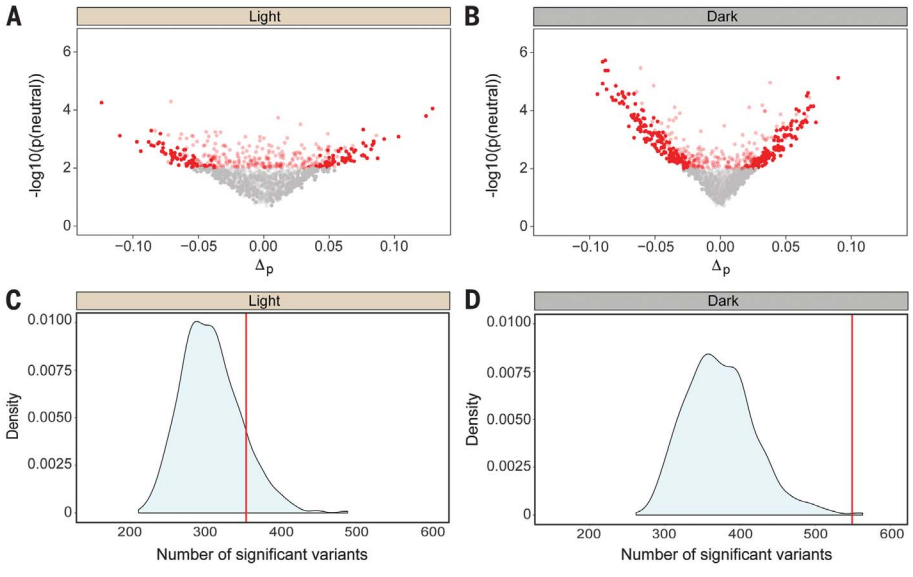

Fig. 3. Allele frequency change at the *Agouti* locus. (**A** and **B**) Allele frequency change from mortality during the experiment in the pooled light (A) and dark (B) enclosures. The *x* axis represents the change in allele frequency between initial colonizing populations and survivors sampled after 3 months. The *y* axis represents the probability of the distribution of genotype frequencies observed in the survivors, assuming a neutral model. All red points are significant at the 1% level: Light red points are significant because of a bias in the observed proportion of heterozygotes, whereas dark red points exhibit a bias in the observed number of homozygotes. (**C** and **D**) Null distributions of the number of sites expected to show significant allele frequency change at the 1% level in the pooled light (C) and dark (D) enclosures. Vertical red lines represent the observed number of sites with significant allele frequency change.

The functional and ecological effects of a deletion mutation in *Agouti*

To test the functional link between one of the variants in *Agouti* associated with survival and pigmentation, as well as uncover the causal molecular mechanism, we focused on the amino acid mutation ΔSer in *Agouti*. We chose this variant because the ΔSer was strongly associated with dorsal brightness ($R^2 = 0.11$, $P < 0.001$) (Fig. 5A), showed a signature of selection in the enclosure populations (Fig. 4A) as well as in an admixed natural population (*15*), and showed the highest level of genetic differentiation across the *Agouti* locus between mice that were originally captured from light and dark habitat ($F_{ST} = 0.34$) (Fig. 4B and table S6). To determine whether the ΔSer mutation alone has an effect on hair color in vivo, we generated matching lines of transgenic lab mice (C57BL/6 mice, a strain with no endogenous *Agouti* expression) carrying the wild-type (WT) or the ΔSer *Peromyscus Agouti* cDNA, constitutively driven by the Hsp68 promoter (Fig. 5B). We used the ϕC31 integrase system, which produces single-copy integrants at the *H11P3* locus on mouse chromosome 11 to directly measure the effect of the *Agouti* ΔSer while avoiding variation caused by copy number, insertion site, or orientation of the construct (*21*) (fig. S3, A and B). Using a spectrophotometer to quantify differences in coat color, we found that ΔSer mice had significantly lighter coats than mice carrying the WT *Peromyscus Agouti* cDNA (ΔSer versus WT, two-tailed *t* test; $n = 5$, $P = 0.001$) (Fig. 5C). Thus, the *Agouti* ΔSer mutation alone has a measurable effect on pigmentation and in the direction expected on the basis of the genotype-phenotype association data in natural *Peromyscus* populations.

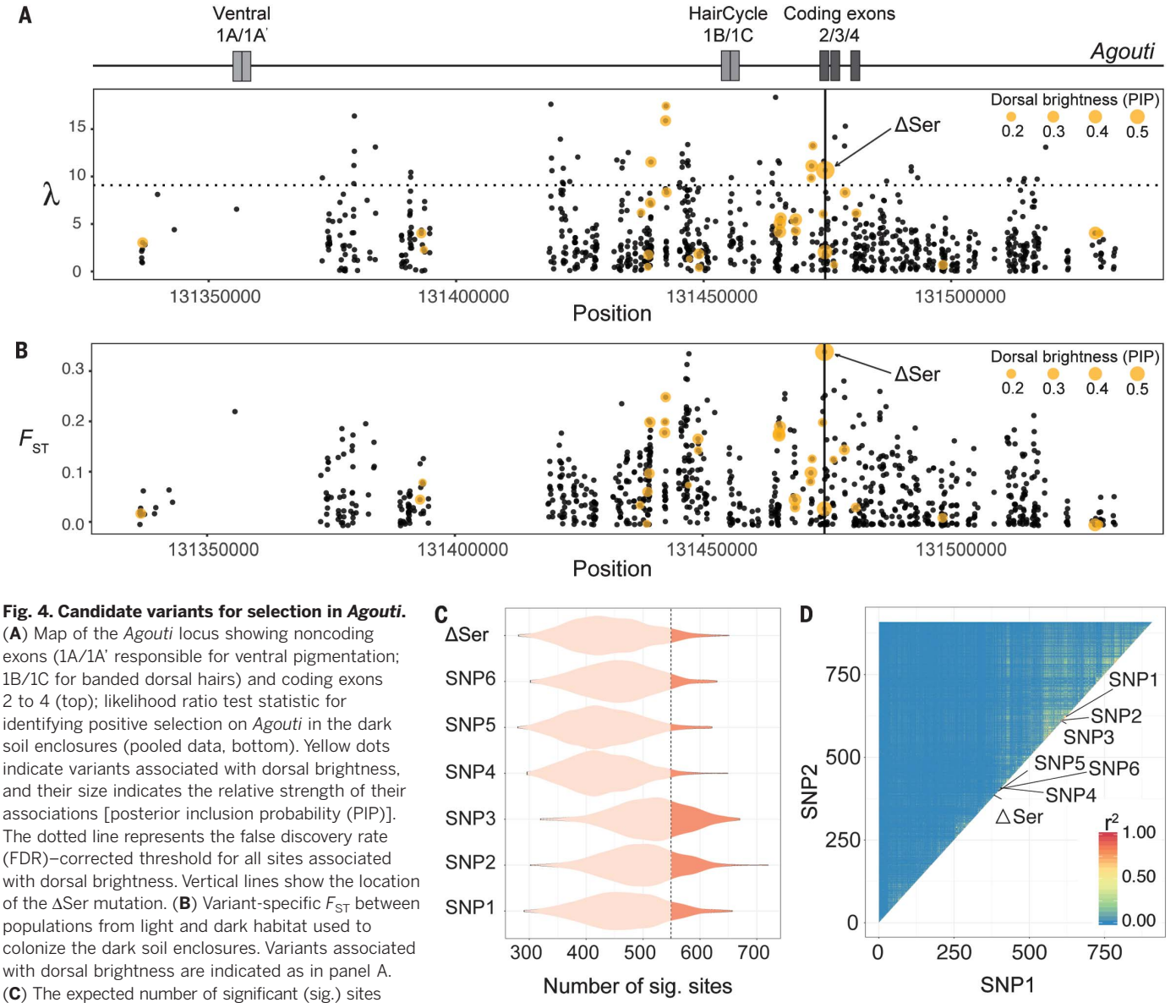

Fig. 4. Candidate variants for selection in *Agouti*. (**A**) Map of the *Agouti* locus showing noncoding exons (1A/1A' responsible for ventral pigmentation; 1B/1C for banded dorsal hairs) and coding exons 2 to 4 (top); likelihood ratio test statistic for identifying positive selection on *Agouti* in the dark soil enclosures (pooled data, bottom). Yellow dots indicate variants associated with dorsal brightness, and their size indicates the relative strength of their associations [posterior inclusion probability (PIP)]. The dotted line represents the false discovery rate (FDR)–corrected threshold for all sites associated with dorsal brightness. Vertical lines show the location of the ΔSer mutation. (**B**) Variant-specific F_{ST} between populations from light and dark habitat used to colonize the dark soil enclosures. Variants associated with dorsal brightness are indicated as in panel A. (**C**) The expected number of significant (sig.) sites when a single site is under selection. Distributions show the number of sites with a *P* value ≤ 0.01 when survivors are artificially resampled assuming a noncentral sampling distribution with weights defined by the genotype at the target site. Distributions are shown for the seven candidate sites in the dark enclosures. The dashed vertical line indicates the observed number of sites with significant change, and the area of the distribution to the right of the dashed line indicates the proportion of resampled datasets with at least as many significant sites as in the observed data (the *P* value). None of the seven *P* values are significant after correcting for multiple testing (FDR). (**D**) LD heat map for all *Agouti* sites in pooled enclosures on dark soil. Sites with a minor allele frequency ≤ 10% were discarded.

To further characterize the phenotypic effects of the ΔSer variant, we examined and then quantified pigment in dorsal hair. Microscopic examination of individual hairs revealed that the hair of ΔSer mice contained a qualitatively lighter pigment than that of WT mice (Fig. 5B). We then analyzed pheomelanin content in the hair by using chemical degradation products followed by high-performance liquid chromatography (HPLC) (*22*–*25*). ΔSer mice had significantly lower amounts of pheomelanin (both benzothiazine and benzothiazole types) than hair from WT mice (ΔSer versus WT, two-tailed *t* test; $n = 5$, $P = 0.002$) (Fig. 5C and fig. S3C). These results indicate that the *Peromyscus* ΔSer causes a decrease in production of pheomelanin, which in turn causes hair to appear brighter overall.

The ΔSer mutation is found in a highly conserved region of the N-terminal domain of the agouti protein, a region that directly binds to attractin, a transmembrane receptor expressed in melanocyte membranes and required for agouti function (*26*). To understand the mechanism by which ΔSer decreases pheomelanin production, we measured real-time binding interactions between the agouti and attractin proteins by using surface plasmon resonance (SPR). In SPR, one molecule (ligand) is immobilized on a sensor surface while a potential interacting partner (analyte) is injected; the reflection angle of polarized light from the sensor then serves as a proxy for the strength of the interaction between the molecules. For a ligand, we used the secreted isoform of natural human Attractin ($ATRN^{Ec}$), and for the analyte, we used a synthetic version of the *Peromyscus* agouti WT or ΔSer N-terminal domain, a region known to retain full biochemical activity and bind attractin (*26*). Application of the WT or ΔSer agouti N-terminal domain to an attractin-coated chip produced sensorgrams characteristic of a biological interaction, approaching equilibrium over several minutes and declining during washout to levels above baseline (Fig. 5D). However, we found that the WT N-terminal domain showed a stronger

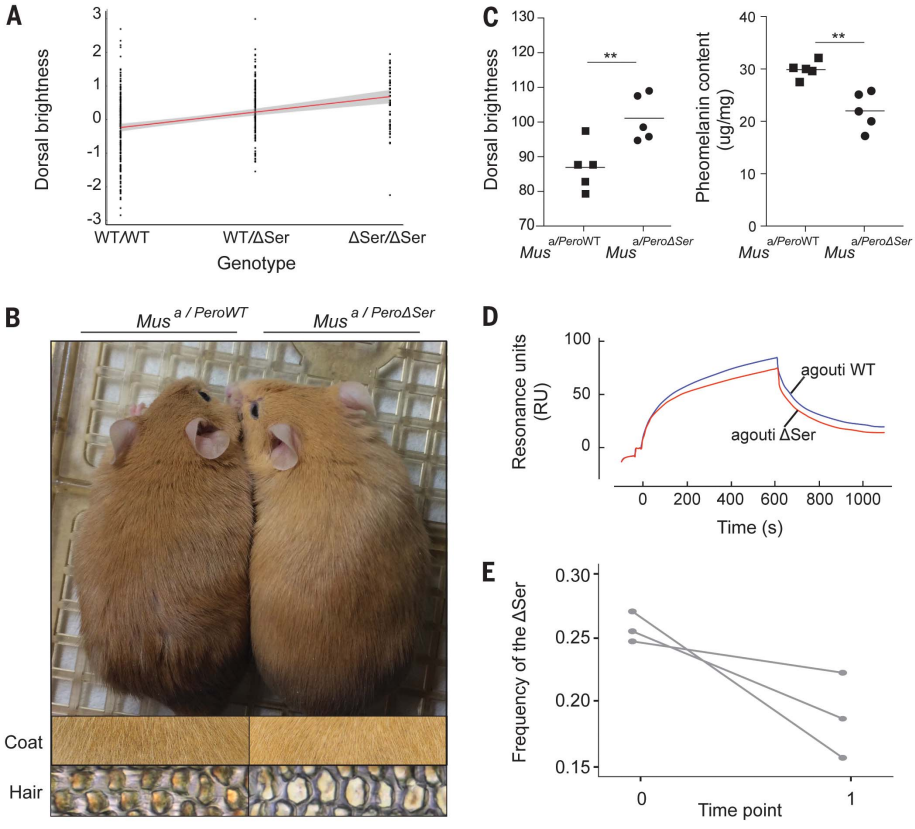

Fig. 5. Phenotypic, molecular, and fitness effects of the serine deletion. (**A**) Linear regression of ΔSer genotypes and dorsal brightness; data pooled across all six enclosures. (**B**) Matched lines of transgenic *Mus* (in C57BL/6, an *Agouti* knockout strain) expressing the WT (dark) or the ΔSer (light) *Peromyscus Agouti* allele. Close-up pictures show the intensity of pheomelanin in dorsal coats and individual dorsal hairs from transgenic mice. (**C**) Dorsal brightness (left) and benzothiazine-type pheomelanin degradation products (right) in the transgenic mice, measured with spectrophotometry and HPLC methods, respectively. (**D**) Biochemical interaction of attractin and the N-terminal domain of the *Peromyscus* WT (blue) or the ΔSer (red) agouti protein. Values shown in arbitrary response units have been corrected for nonspecific binding. (**E**) Changes in $a^{\Delta Ser}$ allele frequency across the three replicate dark enclosure populations. $^{**}P < 0.01$

interaction with attractin relative to the ΔSer allele (Fig. 5D). We next estimated dissociation constants (K_d) by using Scatchard analysis of equilibrium binding levels at different concentrations and showed that the WT domain has a nearly twofold smaller K_d than the ΔSer domain (4.25×10^{-7} versus 6.94×10^{-7}, respectively), consistent with the WT allele having a greater binding affinity to attractin (fig. S3D). Together, our genetic and biochemical experiments indicate that ΔSer causes lighter pigmented hair by decreasing the strength of the interactions with attractin, reducing pheomelanin production, and ultimately increasing the brightness of a mouse's dorsal coat.

Changes in the *Agouti* ΔSer allele through space and time

After verifying its functional role in pigment variation, we next measured the frequency of the *Agouti* ΔSer allele across enclosures and over time. To confirm the *Agouti* ΔSer genotype and to include individuals with missing data, we genotyped all individuals by using a Taqman assay. The starting frequency of the ΔSer allele varied among the six enclosures but on average was similar among dark and light enclosures (light enclosures mean = 29.85 ± 1.80% SE, dark enclosures mean = 25.79 ± 0.68% SE). We observed idiosyncratic changes in allele frequency in the light enclosures, with two of three enclosures showing the expected increases in the ΔSer allele, but the degree of change was minor in all cases (average allele frequency change = 0.43 ± 0.81% SE). By contrast, we observed significant decreases in the ΔSer allele in all three replicate dark enclosures (average allele frequency change = 6.87 ± 2.58% SE) (Fig. 5E). This change in allele frequency amounts to a mean selection coefficient of 0.32 (±0.11 SE; one-sided *t* test of selection coefficients in light versus dark enclosures: $t = 2.990$, df = 2.496, $P = 0.037$) (table S7). As expected given the negative phenotypic selection observed on light pigmentation in dark enclosures, these genetic results provide evidence for negative selection on the ΔSer allele associated with light pigmentation on dark substrates. Thus, by documenting allele frequency change over time, we demonstrate strong selection at the genetic level consistent with predictions based on the functional effects of the ΔSer variant.

Discussion

Knowing the strength of selection in nature is essential to predict rates of adaptive change (*4*, *27*–*31*). We now have extensive data on the strength of selection acting on phenotypes (*32*–*34*) and statistical signatures of historical selection on the genome (*35*–*38*). However, uncertainty remains concerning the magnitude and causes of genetic changes that occur as populations evolve under new ecological conditions (*39*–*42*). Our experimental design mimics the replicated and reciprocal colonization of divergent habitats by populations carrying sequence variants that cause functional changes in a locally adapted phenotype. We demonstrate that when appropriate standing genetic variation is available, natural selection can result in evolutionary change on ecological time scales (*43*). Changes in both our focal trait (dorsal brightness) and components of its underlying genetic architecture (the ΔSer mutation) were predictable from transgenic and biochemical assays as well as patterns of existing phenotypic and genotypic variation across habitat types. Together, these results suggest that knowledge about the functional connections between genotype, phenotype, and fitness could help predict future evolution under defined ecological conditions.

REFERENCES AND NOTES

1. R. Mallarino *et al.*, *Nature* **539**, 518–523 (2016).
2. M. A. Ilardo *et al.*, *Cell* **173**, 569–580.e15 (2018).
3. D. Bradley *et al.*, *Science* **358**, 925–928 (2017).
4. J. G. Kingsolver, S. E. Diamond, A. M. Siepielski, S. M. Carlson, *Evol. Ecol.* **26**, 1101–1118 (2012).
5. O. Lapiedra, T. W. Schoener, M. Leal, J. B. Losos, J. J. Kolbe, *Science* **360**, 1017–1020 (2018).
6. S. K. Auer, C. A. Dick, N. B. Metcalfe, D. N. Reznick, *Nat. Commun.* **9**, 14 (2018).
7. R. A. Bay *et al.*, *Am. Nat.* **189**, 463–473 (2017).
8. R. D. Barrett, H. E. Hoekstra, *Nat. Rev. Genet.* **12**, 767–780 (2011).
9. D. B. Loope, J. Swinehart, *Great Plains Res.* **10**, 5–35 (2000).
10. A. Bleed, *Atlas of the Sand Hills* (University of Nebraska, Omaha, 1990).
11. L. R. Dice, *University of Michigan* **15**, 1–19 (1941).
12. L. Dice, *University of Michigan* **34**, 1–20 (1947).
13. C. R. Linnen, E. P. Kingsley, J. D. Jensen, H. E. Hoekstra, *Science* **325**, 1095–1098 (2009).
14. C. R. Linnen *et al.*, *Science* **339**, 1312–1316 (2013).
15. S. P. Pfeifer *et al.*, *Mol. Biol. Evol.* **35**, 792–806 (2018).
16. M. Manceau, V. S. Domingues, C. R. Linnen, E. B. Rosenblum, H. E. Hoekstra, *Philos. Trans. R. Soc. Lond. B Biol. Sci.* **365**, 2439–2450 (2010).
17. Y. Chen, D. M. J. Duhl, G. S. Barsh, *Genetics* **144**, 265–277 (1996).
18. See supplementary materials.
19. R. H. Baker, *Michigan Mammals* (Wayne State Univ., Detroit, 1983).
20. V. S. Domingues *et al.*, *Evolution* **66**, 3209–3223 (2012).
21. B. Tasic *et al.*, *Proc. Natl. Acad. Sci. U.S.A.* **108**, 7902–7907 (2011).
22. K. Wakamatsu, S. Ito, J. L. Rees, *Pigment Cell Res.* **15**, 225–232 (2002).
23. S. Ito *et al.*, *Pigment Cell Melanoma Res.* **24**, 605–613 (2011).
24. M. d'Ischia *et al.*, *Pigment Cell Melanoma Res.* **26**, 616–633 (2013).
25. S. Del Bino *et al.*, *Pigment Cell Melanoma Res.* **28**, 707–717 (2015).
26. L. He *et al.*, *Nat. Genet.* **27**, 40–47 (2001).
27. P. R. Grant, B. R. Grant, *Evolution* **49**, 241–251 (1995).
28. P. Nosil *et al.*, *Science* **359**, 765–770 (2018).
29. M. Bosse *et al.*, *Science* **358**, 365–368 (2017).
30. R. Fisher, *The Genetical Theory of Natural Selection* (Oxford Univ. Press, 1930).
31. R. Bürger, M. Lynch, *Evolution* **49**, 151–163 (1995).

32. J. G. Kingsolver *et al*., *Am. Nat.* **157**, 245–261 (2001).
33. A. M. Siepielski, J. D. DiBattista, S. M. Carlson, *Ecol. Lett.* **12**, 1261–1276 (2009).
34. A. M. Siepielski *et al*., *Ecol. Lett.* **16**, 1382–1392 (2013).
35. M. Nei, Y. Suzuki, M. Nozawa, *Annu. Rev. Genomics Hum. Genet.* **11**, 265–289 (2010).
36. R. Nielsen, *Annu. Rev. Genet.* **39**, 197–218 (2005).
37. J. D. Jensen, M. Foll, L. Bernatchez, *Mol. Ecol.* **25**, 1–4 (2016).
38. T. J. Thurman, R. D. H. Barrett, *Mol. Ecol.* **25**, 1429–1448 (2016).
39. P. Librado *et al*., *Proc. Natl. Acad. Sci. U.S.A.* **112**, E6889–E6897 (2015).
40. Y. Kim, D. Gulisija, *Genetics* **184**, 571–585 (2010).
41. G. S. Bradburd, P. L. Ralph, G. M. Coop, *Evolution* **67**, 3258–3273 (2013).
42. S. Peischl *et al*., *Genetics* **208**, 763–777 (2018).
43. A. P. Hendry, *Eco-evolutionary dynamics* (Princeton Univ. Press, Princeton, 2017).
44. R. D. H. Barrett, *et al*., Data from: Linking a mutation to survival in wild mice, Dryad Digital Repository (2018); doi:10.5061/dryad.60mk699.
45. R. D. H. Barrett, L. K. M'Gonigle, mouse-recapture-v1.0.0, Version 1.0.0, Zenodo (2018); doi:10.5281/zenodo.1758243.
46. S. Badion, S. Laurent, rsurvival-0.1.0, Version 0.1.0, Zenodo (2018); doi:10.5281/zenodo.1753895.

ACKNOWLEDGMENTS

We thank F. Baier, N. Bedford, A. Bendesky, J. Best, J. Chu, C. Clabaut, J. Gable, E. Hager, G. Hood, E. Jacobs-Palmer, E. Kay-Delaney, E. Kingsley, J. Kwon, M. Manceau, N. Man in't Veld, H. Metz, J.-M. Lassance, E. Lievens, C. Linnen, N. Rubinstein, L. Schmitt, H. Wegener, and I. Yen for field assistance; C. Clabaut, P. Muralidhar, and K. Turner for laboratory assistance; Z. Gompert, B. Peterson, and J.-M. Lassance for bioinformatics assistance; S. Badion for programming assistance; J. Demboski, B. Perrett, M. Perrett, B. Peterson, J. Ramos, L. Ramos, B. Ward, J. Wasserman, R. Wasserman, and the Denver Museum of Nature and Science for logistical support; L. M'Gonigle for assistance with capture-recapture analysis; and J. Chupasko for curatorial assistance. We thank G. Barsh, J. Losos, P. Nosil, D. Petrov, D. Schluter, and T. Thurman for commenting on the manuscript. **Funding:** R.D.H.B. was supported by a Natural Sciences and Engineering Research Council of Canada Banting Postdoctoral Fellowship, a Foundational Questions in Evolutionary Biology Postdoctoral Fellowship, and a Canada Research Chair. C.C.Y.X. was supported by a Vanier Canada Graduate Scholarship from the Natural Sciences and Engineering Research Council of Canada. S.L., M.F., and R.M., as well as laboratory work, were supported by a Swiss National Science Foundation Sinergia grant to J.D.J, H.E.H., and L. Excoffier. Fieldwork was funded by the National Geographic Society, Putnam Expedition Grants from the Harvard Museum of Comparative Zoology (MCZ), and a Discovery Grant from the National Engineering and Research Council of Canada to R.D.H.B. H.E.H. is an Investigator of the Howard Hughes Medical Institute. **Author contributions:** R.D.H.B. conceived the study. R.D.H.B and H.E.H. designed and led the project. R.D.H.B. conducted the field experiment with C.C.Y.X. R.D.H.B conducted the phenotypic analyses and collected genomic data. S.P.P. and S.L. conducted the bioinformatics analyses. R.D.H.B., S.L., M.F., and J.D.J. conducted the statistical analyses. R.M. conducted the functional experiments, including the protein experiments with J.S.D.-C. and the melanin analysis with K.W. R.D.H.B. drafted the manuscript with major input from S.L., R.M., and H.E.H. All authors contributed revisions and approved the final version of the manuscript. **Competing interests:** The authors declare no competing financial interests. **Data and materials availability:** We have deposited sampling, phenotype, and survival data in the Dryad Digital Repository (*44*) and sequence data in the NCBI Short Read Archive with the primary accession code SUB4114786. The R code implementing capture-recapture analyses is available from https://doi.org/10.5281/zenodo.1758243 (*45*). The R code implementing analyses of genotype distributions is available from https://doi.org/10.5281/zenodo.1758243 (*46*).

SUPPLEMENTARY MATERIALS

www.sciencemag.org/content/363/6426/499/suppl/DC1
Materials and Methods
Supplementary Text
Figs. S1 to S3
Tables S1 to S9
References (*47*–*64*)

25 September 2018; accepted 6 December 2018
10.1126/science.aav3824